Cover Sheet

Final Report: DURIP FA9550-05-1-0270

Project Title: Field Emission Gun Scanning Electron Microscopy with Electron Back Scatter Diffraction for Texture, Formability and Fatigue Studies of Advanced Materials

PI: Dr. Tongguang Zhai

Department of Chemical and Materials Engineering
University of Kentucky
177 Paul F. Anderson Tower
Lexington, KY 40506

co-PIs: Chi-Sing Man

Department of Mathematics
University of Kentucky

co-PI: James Morris
Department of Chemical and Materials Engineering
University of Kentucky
177 Paul F. Anderson Tower
Lexington, KY 40506

Agreement no: FA9550-05-1-0270

REPORT DOCUMENTATION PAGE

Form Approved
OMB No. 0704-0188

PLEASE DO NOT RETURN YOUR FORM TO THE ABOVE ORGANIZATION.

1. REPORT DATE *(DD-MM-YYYY)*	2. REPORT TYPE	3. DATES COVERED *(From - To)*
31-05-2007	Final Report	05/01/2005-02/28/2007

4. TITLE AND SUBTITLE

DURIP: Field Emission Gun Scanning Electron Microscopy with Electron Back Scatter Diffraction for Texture, Formability and Fatigue Studies of Advanced Materials

5a. CONTRACT NUMBER

FA9550-05-1-0270

5b. GRANT NUMBER

5c. PROGRAM ELEMENT NUMBER

6. AUTHOR(S)

Tongguang Zhai, Chi-Sing-Man and James Morris

5d. PROJECT NUMBER

5e. TASK NUMBER

5f. WORK UNIT NUMBER

7. PERFORMING ORGANIZATION NAME(S) AND ADDRESS(ES)

University of Kentucky
177 Paul F. Anderson Tower
Lexington, KY 40506

8. PERFORMING ORGANIZATION REPORT NUMBER

9. SPONSORING/MONITORING AGENCY NAME(S) AND ADDRESS(ES)

Carmelita B. Calvert
US Air Force Office of Scientific Research
875 N. Randolph ST., Room 3112
Arlington, VA22203

10. SPONSOR/MONITOR'S ACRONYM(S)

11. SPONSOR/MONITOR'S REPORT NUMBER(S)

AFRL-SR-AR-TR-08-0497

12. DISTRIBUTION/AVAILABILITY STATEMENT

Distribution A: Unlimited distribution for public release.

13. SUPPLEMENTARY NOTES

14. ABSTRACT

An advanced field emission gun scanning electron microscope (FEGSEM Hitachi S-4300) equipped with energy dispersion spectroscopy (EDS PGT Spirit, presently a part of Bruker) and electron back scatter diffraction (EBSD HKL Channel 5, presently a part of Oxford Instruments) was acquired by the support jointly from AFOSR ($250,000) through a DURIP program and the University of Kentucky ($161,365). The FEGSEM-EDS-EBSD system was installed in July 2006 and has been used in one DoD-funded project and two other research projects that are of interest to the Department of Defense, and in materials education at the University of Kentucky.

15. SUBJECT TERMS

16. SECURITY CLASSIFICATION OF:			17. LIMITATION OF ABSTRACT	18. NUMBER OF PAGES	19a. NAME OF RESPONSIBLE PERSON
a. REPORT	b. ABSTRACT	c. THIS PAGE			19b. TELEPHONE NUMBER *(Include area code)*

Reset

INSTRUCTIONS FOR COMPLETING SF 298

1. REPORT DATE. Full publication date, including day, month, if available. Must cite at least the year and be Year 2000 compliant, e.g. 30-06-1998; xx-06-1998; xx-xx-1998.

2. REPORT TYPE. State the type of report, such as final, technical, interim, memorandum, master's thesis, progress, quarterly, research, special, group study, etc.

3. DATES COVERED. Indicate the time during which the work was performed and the report was written, e.g., Jun 1997 - Jun 1998; 1-10 Jun 1996; May - Nov 1998; Nov 1998.

4. TITLE. Enter title and subtitle with volume number and part number, if applicable. On classified documents, enter the title classification in parentheses.

5a. CONTRACT NUMBER. Enter all contract numbers as they appear in the report, e.g. F33615-86-C-5169.

5b. GRANT NUMBER. Enter all grant numbers as they appear in the report, e.g. AFOSR-82-1234.

5c. PROGRAM ELEMENT NUMBER. Enter all program element numbers as they appear in the report, e.g. 61101A.

5d. PROJECT NUMBER. Enter all project numbers as they appear in the report, e.g. 1F665702D1257; ILIR.

5e. TASK NUMBER. Enter all task numbers as they appear in the report, e.g. 05; RF0330201; T4112.

5f. WORK UNIT NUMBER. Enter all work unit numbers as they appear in the report, e.g. 001; AFAPL30480105.

6. AUTHOR(S). Enter name(s) of person(s) responsible for writing the report, performing the research, or credited with the content of the report. The form of entry is the last name, first name, middle initial, and additional qualifiers separated by commas, e.g. Smith, Richard, J, Jr.

7. PERFORMING ORGANIZATION NAME(S) AND ADDRESS(ES). Self-explanatory.

8. PERFORMING ORGANIZATION REPORT NUMBER. Enter all unique alphanumeric report numbers assigned by the performing organization, e.g. BRL-1234; AFWL-TR-85-4017-Vol-21-PT-2.

9. SPONSORING/MONITORING AGENCY NAME(S) AND ADDRESS(ES). Enter the name and address of the organization(s) financially responsible for and monitoring the work.

10. SPONSOR/MONITOR'S ACRONYM(S). Enter, if available, e.g. BRL, ARDEC, NADC.

11. SPONSOR/MONITOR'S REPORT NUMBER(S). Enter report number as assigned by the sponsoring/ monitoring agency, if available, e.g. BRL-TR-829; -215.

12. DISTRIBUTION/AVAILABILITY STATEMENT. Use agency-mandated availability statements to indicate the public availability or distribution limitations of the report. If additional limitations/ restrictions or special markings are indicated, follow agency authorization procedures, e.g. RD/FRD, PROPIN, ITAR, etc. Include copyright information.

13. SUPPLEMENTARY NOTES. Enter information not included elsewhere such as: prepared in cooperation with; translation of; report supersedes; old edition number, etc.

14. ABSTRACT. A brief (approximately 200 words) factual summary of the most significant information.

15. SUBJECT TERMS. Key words or phrases identifying major concepts in the report.

16. SECURITY CLASSIFICATION. Enter security classification in accordance with security classification regulations, e.g. U, C, S, etc. If this form contains classified information, stamp classification level on the top and bottom of this page.

17. LIMITATION OF ABSTRACT. This block must be completed to assign a distribution limitation to the abstract. Enter UU (Unclassified Unlimited) or SAR (Same as Report). An entry in this block is necessary if the abstract is to be limited.

Final Report

Objective: no change.
The main objective of this project was to acquire an advanced FEGSEM-EDS-EBSD system to support macro- and micro-texture, nano-scale imaging and composition analysis experiments for the research that is of interest to the Department of Defense.

Status of Effort

As shown in Fig. 1, an advanced field emission gun scanning electron microscope (Hitachi S-4300 FEG-SEM) equipped with energy dispersion spectroscopy (PGT Spirit EDS, presently a part of Bruker Company) and electron back scatter diffraction (HKL Channel 5 EBSD, presently a part of Oxford Instruments) was acquired by the support jointly from AFOSR ($250,000) through a DURIP program and the University of Kentucky ($161,365). The FEGSEM-EDS-EBSD system was purchased for $400,000, and the other costs, including lab renovation, materials and supplies, and the indirect charges, were $11,365. The system was installed in July 2006 and has been tested and adjusted over the next 12 months. The system has now been fully functioning and, so far, used in one DoD-sponsored project and two other research projects that are of interest to the Department of Defense, and in materials education at the University of Kentucky.

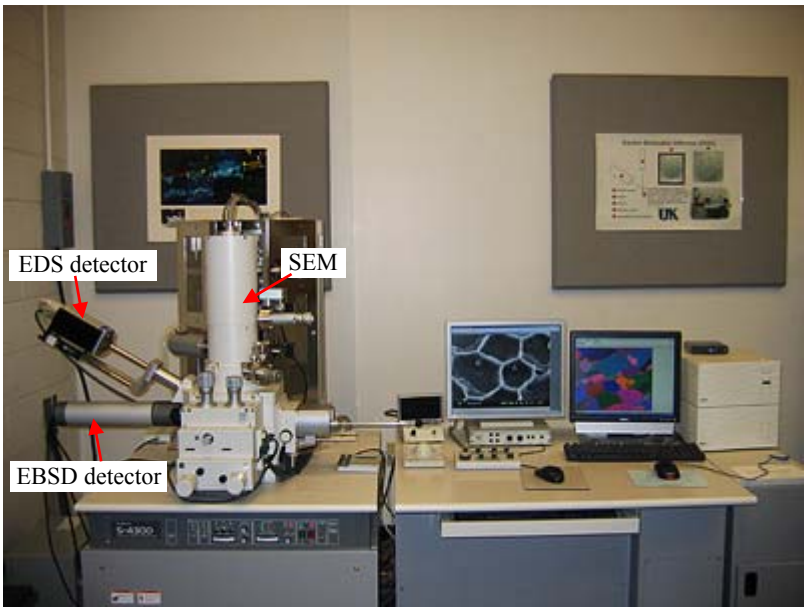

Fig. 1. Hitachi S-4300 FEG-SEM, PGT Spirit EDS and HKL Channel 5 EBSD acquired by the support jointly from AFOSR (DURIP) and University of Kentucky.

Accomplishments/new findings

The main objective of this project was to acquire an advanced FEGSEM-EDS-EBSD system to support macro- and micro-texture, nano-scale imaging and composition analysis experiments for the research that is of interest to the Department of Defense. Since this system was installed, it has been employed in three research projects, including the one sponsored by US Air Force through a DEPSCoR program (FA9550-04-1-0457), and two others in which the materials (50Mo-50Re, Al-Cu and Al-Li alloys) studied are often used in defense related applications. This equipment has also been used in several materials courses including MSE436 (failure analysis), MSE480 (materials design) and MSE585 (materials characterization) at the University of

Kentucky. The research work done recently on these materials using the FEGSEM-EDS-EBSD system is highlighted as bellow.

Formation of P texture component ({011}⟨566⟩)

This work is part of a DEPSCoR-AFOSR project, "Prediction of Texture and Formability of Continuous Cast AA 5000, 3000, and 2000 Series Aluminum Alloy Sheet and Their Quality Improvement"

PI: Eric Grulke (originally James G. Morris, passed away in 2006),
co-PIs:Chi-Sing Man, and Tony Zhai
DEPSCoR/AFOSR, Agreement No: FA9550-04-1-0457 (06/01/2004 - 08/31/08)
Program Manager: Dr. Brett Conner

The main aims of this DEPSCoR/AFOSR-funded research project are:

- Developing continuous cast 2000 series aluminum alloys for potential use in aerospace applications,
- Prediction of the evolution of crystallographic texture in continuous cast AA 5000, 3000, and 2000 series aluminum alloys during cold rolling and annealing respectively.

AA3004 Al alloys used in this project were produced by the continuous cast (CC) technology using a Hazelett strip caster. The CC technology presents an energy savings of at least 25 percent and an economic savings of more than 14 percent over sheet made from conventional direct chill cast ingots. However, the alloys produced by the continuous cast technology often show an inferior formability, compared to the alloys produced by conventional direct chill casting (DC). A strong P texture component {011}⟨566⟩ is often formed in recrystallized CC Al alloys, especially in 3000 series Al alloys [1-3]. It has been recognized that, in a DC Al-Mn alloy, the P component is formed due to the concurrent precipitation effect, i.e., precipitation of Al_6Mn upon heating of the deformed and supersaturated alloy [4,5]. The concurrent precipitation retards the recrystallization process by pinning dislocations during annealing. Rotation of deformation orientations (e.g., about ⟨011⟩ axis of brass orientation {011}⟨211⟩) at a temperature higher than the usual recrystallization temperature for the same alloy with a low solid solution level leads to nucleation of P oriented grains ({011}⟨566⟩). And the preferred growth of the P oriented grains is responsible for the formation of a strong P component in the recrystallized Al-Mn alloy.

It is still desirable to study the formation mechanism of the P orientation, and its effect on mechanical properties in CC Al alloys, since CC Al alloy hot band shows a high level of supersaturation due to their higher cooling rate during solidification. The high level of supersaturation could lead to the formation of strong P texture due to precipitation occurring during subsequent thermomechanical treatment. As part of an effort to understand the formation mechanism of P orientation and the interaction between precipitates and dislocations, EBSD experiments were conducted to study the formation of P texture component in a CC AA3004 Al alloy, in this project. It was found that a strong P orientation could also be formed without the occurrence of concurrent precipitation but by producing a large number of Al_6Mn precipitates prior deformation and annealing in CC AA3004 Al alloys.

In this work, in order to avoid occurrence of concurrent precipitation during annealing, the CC AA3004 Al alloy hot band was first annealed at 420^{o}C for 4 hours to minimize its supersaturation level. Then, it was cold rolled by 85% reduction and subsequently annealed. As shown in Fig. 2, EBSD measurement (in texture component mapping) by the newly acquired

FEGSEM-EDS-EBSD system showed that P oriented grains could overgrow most of the nucleated grains with other orientations in the early stage of the recrystallization process (Fig. 2(a)) and that the P grains were coarse and elongated after full recrystallization (Fig. 2(b)).

The main results obtained from this project include 1) identification of formation mechanism for P orientation in CC Al alloys, 2) the maximum volume fraction of P component could be obtained by pre-annealing the hot band of the alloy followed by cold rolling and annealing, 3) formation of P texture led to inferior formability, and minimization of P texture formation could be achieved by either faster heating or pre-annealing for a prolonged period of time. These results are of value for Al industry to improve the formability and quality of the final CC aluminum products, and also provide the sound scientific know-how to design new CC aluminum alloys.

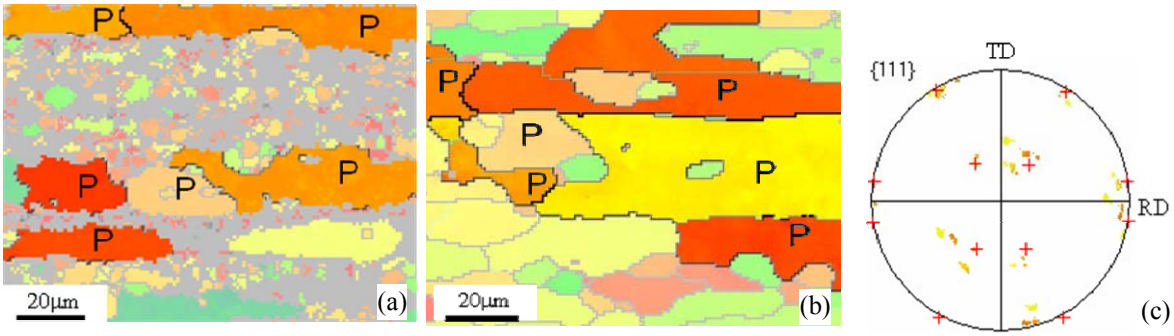

Fig. 2. A CC AA3004 Al alloy pre annealed at 420°C, 85% cold rolled, and annealed. Texture component contrast by EBSD measurement: (a) partially recrystallized, showing P oriented grains overgrow grains with other orientations, (b) fully recrystallized with P oriented grains being coarse and elongated, and (c) 111 pole figure showing the position of the P oriented grains and the standard P orientation (red cross).

Imaging local plastic deformation in 50Mo-50Re alloys with electron back scatter diffraction (EBSD)

Refractory metal molybdenum alloyed with rhenium is used in many applications such as heating elements, thermocouple sheathings, vacuum furnace components, electron tube components, satellites, space nuclear reactor and space shuttle applications due to its high melting temperature and high strength [6,7]. The strength, creep resistance, and low temperature ductility of W, Mo, Cr metals are all improved with increasing the rhenium content up to its solubility limit [8]. The yield strength and ultimate tensile strength of commercially available molybdenum are 300 MPa and 350 MPa respectively at ambient temperature, as compared to 845 MPa and 1053 MPa respectively for the molybdenum alloy with a rhenium content of 47.5 wt% (so-called 50Mo-50Re) in the fully annealed condition [9]. The elongation of pure Mo is 4.1% [10], while that of this alloy can reach 19% at room temperature [8].

Recently, the PI's group has discovered that 50Mo-50Re alloy sheet shows anomalous strain rate dependence that its elongation is increased significantly by increasing the strain rate [11]. It is desirable to understand the mechanism for this anomalous dependence in terms of its deformation and fracture behaviors. In this work, the deformation behavior in a fully-recrystallized 50Mo-50Re alloy was studied after tensile deformation using EBSD, together with scanning electron microscope (SEM) and transmission electron microscope (TEM). As shown in Fig. 3, it was found that there was usually a large misorientation gradient close to a grain boundary triple junction in deformed 50Mo-50Re alloys (Fig. 3(b)), as revealed by EBSD

measurement. Fig. 3(c) shows the profile of misorientation and its gradient along the line shown in Fig. 3(b). The misorientation gradient is related to local strain, though there is still a lack of quantitative relation between them [12]. The revelation of high misorientation gradient occurring close to grain boundary triple junctions during deformation was consistent with observation of crack nucleation at grain boundary triple junctions in this alloy, as demonstrated in Fig. 4. Our recent TEM observation of the deformed 50Mo-50Re alloy also revealed high lattice rotation taking place close to grain boundaries. It was also found in this project that cracking enhanced toughness of this alloy. Further work needs to be done to understand the mechanisms for these observed phenomena, in order to help design new alloys that possess similar strain rate dependence and fracture toughening ability. Such alloys would allow higher production efficiency in forming operation and provide higher damage tolerance for key engineering systems.

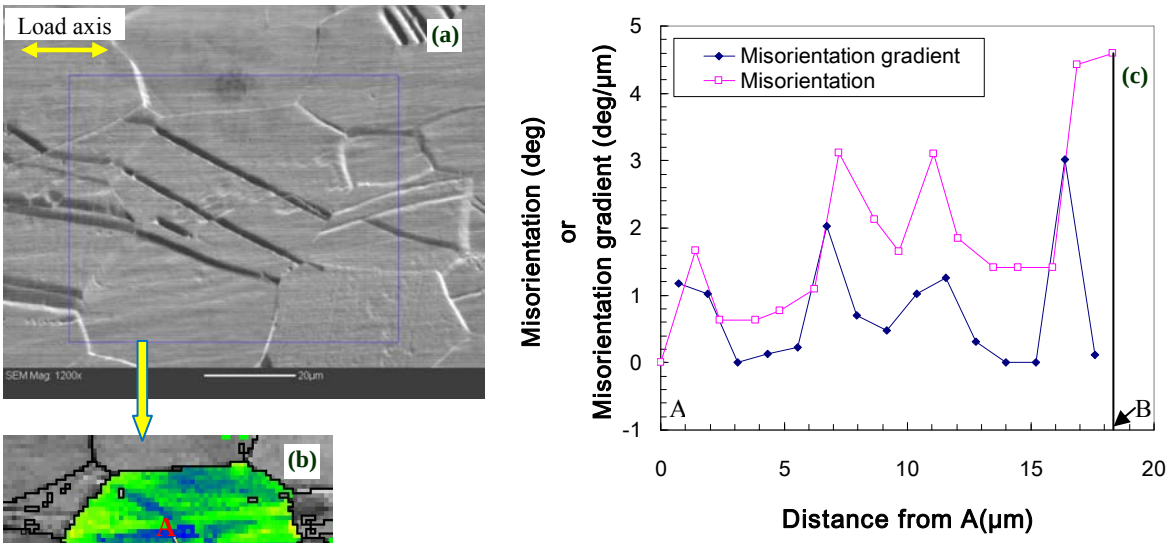

Fig. 3. (a) SEM image of an individual grain on the fully-recrystallized sample; (b) Misorientation map (rainbow scale: blue represents 0º misorientation from reference and red represents 8º misorientation from reference) with band contrasts and grain boundaries (black lines are high angle [θ >10º] boundaries); (c) Misorientation angle and misorientation gradient profiles along a line from point A to point B shown in (b).

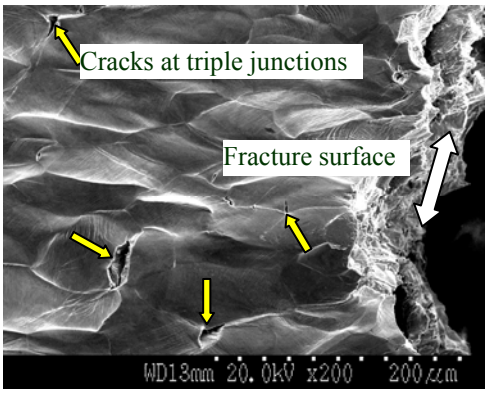

Fig. 4. SEM micrograph showing crack nucleation at grain boundary triple junctions on the surface of the fully-recrystallized 50Mo-50Re alloy after tensile test.

Prediction of short fatigue crack growth in Al-Cu and Al-Li alloys

The newly acquired FEGSEM-EDS-EBSD system has also been used in a study of short fatigue crack growth in new generation AA2026 Al-Cu and AA2099 Al-Li alloys obtained from Alcoa Inc [13-15]. These alloys show superior high cycle fatigue properties, almost doubling their fatigue strength compared to those of their predecessors. In this project, fatigue cracks were found to propagate in the direction of about 30° relative to the extrusion axis which was also the loading axis. As shown in Fig. 5, the EBSD experiments revealed that the alloys had two distinct regions, one being about 80% volume fraction and having typical rolling texture (i.e., β fiber texture), and the other having typical recrystallized texture. As shown in Fig. 6(a), within the deformation textured regions, a crack was straight and crystallographic in the direction of 30° relative to the extrusion axis. In contrast, the crack propagated almost perpendicularly to the extrusion direction in the recrystallized regions. It was found that the crack path within the deformation textured region was controlled by the twist angle of crack plane deflection at each grain boundary that the crack interacted with. The crack selected the slip plane that had the minimum twist angle with the crack plane across the grain boundary. Table 1 shows the tilt angles of the crack path and twist angles of crack plane deflection, quantified from the EBSD measurement, at grain boundaries along the crack segment marked by the line in Fig. 6(b). The twist angles predominantly appeared to be small, and the corresponding crack path was consistent with the observed one within each grain measured.

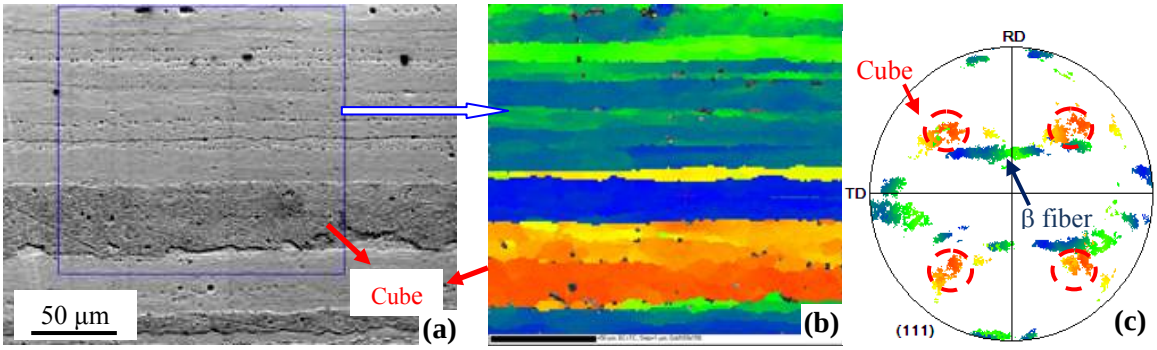

Fig. 5. (a) SEM micrograph of the grain structure on longitudinal-short transverse plane in the AA2099 Al-Li alloy, (b) the EBSD texture component (orientation) map of the same area as marked in (a). (c) the corresponding ⟨111⟩ pole figure obtained from the EBSD measurement, of the same area as in (b).

In this project, it was also found that there was a gradual change in orientation within each grain in this alloy, as shown Fig. 6(c) where the crystallographic orientation changed gradually within grains 3, 4, 5 and 6 respectively. Built on the success in identifying the key factors (tilt and twist angles) that control the crack growth path across grain boundaries, effort is being made by the PI to quantify the growth behavior of a short crack in high performance alloys.

Summary

- Hitachi S-4300 FEG-SEM, PGT Spirit EDS and HKL Channel 5 EBSD were acquired by the support jointly from AFOSR (DURIP) and University of Kentucky.
- The SEM-EDS-EBSD system has, so far, been used in a DOD sponsored project, and research work on alloys that are often used in defense related applications.
- The SEM-EDS-EBSD system has also been actively used in materials education at University of Kentucky.

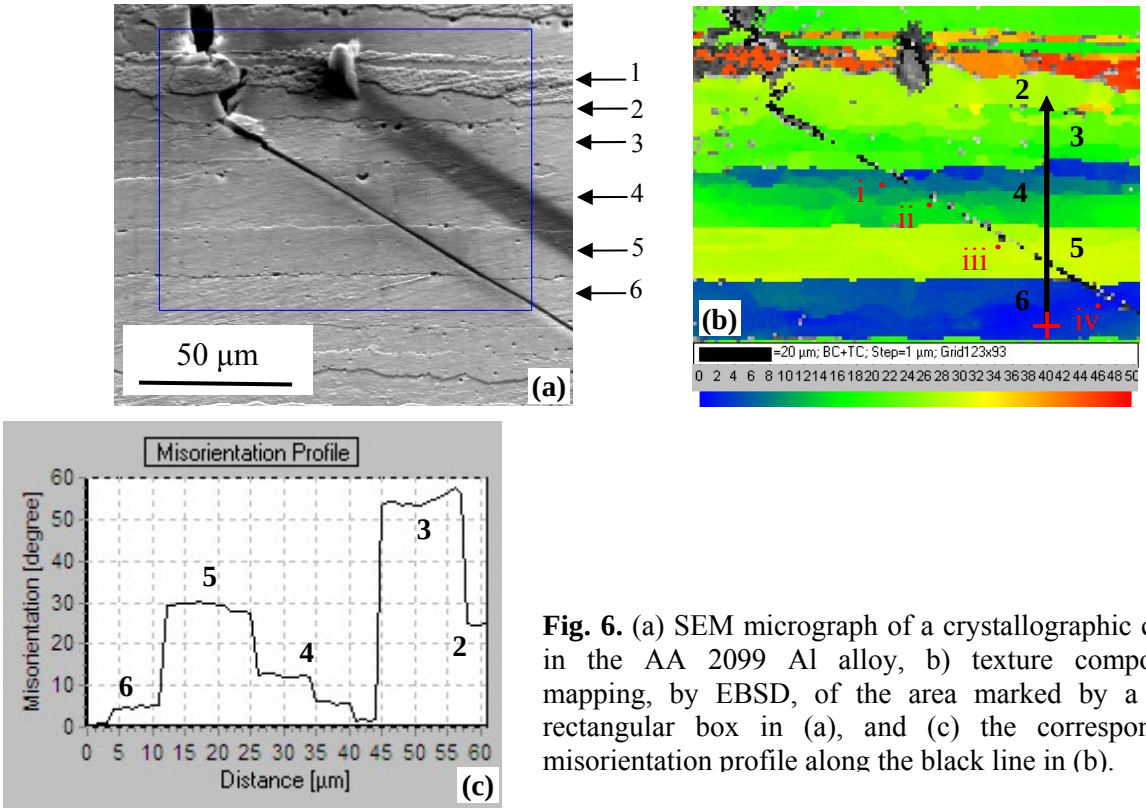

Fig. 6. (a) SEM micrograph of a crystallographic crack in the AA 2099 Al alloy, b) texture component mapping, by EBSD, of the area marked by a blue rectangular box in (a), and (c) the corresponding misorientation profile along the black line in (b).

Table 1. The orientation matrixes of the grains shown in Figure 5 (b), the predicted path of crack growth, and twist angles calculated at their boundaries. θ is the angle between crack path and extrusion direction.

Points	Orientation matrix	Slip planes	Predicted θ	Observed θ	Twist angle α
i	$\begin{pmatrix} -0.418 & -0.213 & -0.883 \\ 0.727 & -0.661 & -0.185 \\ -0.544 & -0.720 & 0.431 \end{pmatrix}$	111 $\bar{1}11$ $1\bar{1}1$ $11\bar{1}$	8.4° ***27.25°*** 80.87° 79.77°	***30°***	
ii	$\begin{pmatrix} -0.387 & -0.292 & -0.875 \\ 0.787 & -0.599 & -0.149 \\ -0.480 & -0.746 & 0.461 \end{pmatrix}$	111 $\bar{1}11$ $1\bar{1}1$ $11\bar{1}$	2.82° ***33.37°*** 75.15° 80.66°	***30°***	19.88° ***2.239°*** 52.86° 121.3°
iii	$\begin{pmatrix} -0.470 & -0.581 & 0.665 \\ -0.402 & -0.530 & -0.747 \\ 0.786 & -0.618 & 0.016 \end{pmatrix}$	111 $\bar{1}11$ $1\bar{1}1$ $11\bar{1}$	2.85° 56.42° ***46.98°*** 73.47°	***30°***	22.08° 118.2° ***3.623°*** 56.31°
iv	$\begin{pmatrix} -0.444 & -0.165 & -0.881 \\ 0.707 & -0.669 & -0.231 \\ -0.551 & -0.725 & 0.413 \end{pmatrix}$	111 $\bar{1}11$ $1\bar{1}1$ $11\bar{1}$	10.47° ***26.04°*** 82.58° 82.41°	***30°***	4.255° ***2.793°*** 55.44° 125.3°

References

[1] J. Li, W.C. Liu, T. Zhai, E. A. Kenik, "Copmarison of Recrystallization Texture in Cold-Rolled Continuous Cast AA5083 and 5182 Aluminum Alloys", Scripta Materiala, 2004; 52/3: 163-168.

[2] X.F. Yu, X.Y. Wen, Y. M. Zhao, T. Zhai, "A Study of Mechanical Isotropy of Continuous Cast and Direct Chill Cast AA5182 Al Alloys", Mater. Sci Eng. A, 2004; Vol. 394, pp. 376-384.

[3] J.G. Morris, W.C. Liu, "Al alloys: The influence of concurrent precipitation on recrystallization behavior, kinetics, and texture" JOM, vol. 57, 2005, pp. 44-47.

[4] Sjolstad, Knut; Engler, Olaf; Tangen, Stian; Marthinsen, Knut; Nes, Erik, "Recrystallization textures and the evolution of the P-orientation as a function of precipitation in an AA3103 alloy", Materials Science Forum, v 408-412, 2002, pp. 1471-1476.

[5] F. J. Humphreys and M. Hatherly: ' Recrystallization and related annealing phenomena ', 2nd edn, 285-378; 2004, Elsevier.

[6] J.T. Busby, K.J. Leonard, S.J. Zinkle, "Radiation-Damage in Molybdenum-Rhenium Alloys for Space Reactor Applications," Journal of Nuclear Materials, Vol. 366, 2007, pp. 388-406.

[7] T. Leonhardt, J.C. Carlen, M. Buck, C.R. Brinkman, W. Ren, C.O. Stevens, Space Technology and Applications, International Forum, AIP Conference Proceedings 458, ed. M.S.El-Genk, 1999, 685.

[8] G.A. Geach, J.E. Hughes, 2nd Plansee Seminar, ed. F. Benesovsky, Pergamon, London, 1956, 245.

[9] J.A. Sheilds, Adv. Powder Metall. Particulate Mater. 8 (1992) 199.

[10] Metal Handbook, Vol.2, 10th edition. Metals Park, OH: ASM International, 1990. p. 557.

[11] J. Xu, T. Leonhardt, J. Farrell, M. Effgen, T. Zhai, "Anomalous strain rate effect on plasticity of a Mo-Re alloy at room temperature", Materials Science and Engineering A, Vol. 479, 2008, pp. 76-82.

[12] M. Kamaya, A.J. Wilkinson, J.M. Titchmarsh, "Quantification of plastic strain of stainless steel and nickel alloy by electron backscatter diffraction", Acta Materialia 54 (2006) 539-548.

[13] J.X. Li, PhD Thesis, University of Kentucky, 2007.

[14] J.X. Li, T. Zhai, M.D. Garratt, G.H. Bray, Four point bend fatigue of AA 2026 Al alloys, Metallurgical and Materials Transaction A, Vol. 36A, 2005, pp. 2529-2539.

[15] X.P, Jiang, PhD Thesis, University of Kentucky, 2007.